Journal of Alloys and Compounds 509 (2011) 8327–8332

Contents lists available at ScienceDirect

Journal of Alloys and Compounds

journal homepage: www.elsevier.com/locate/jallcom

Microstructure and properties of W–ZrC composites prepared by the displacive compensation of porosity (DCP) method

Shouming Zhang*, Song Wang, Wei Li, Yulin Zhu, Zhaohui Chen

Key Lab of Advanced Ceramic Fibers & Composites, College of Aerospace & Materials Engineering, National University of Defense Technology, DeYa Road, Changsha 410073, PR China

ARTICLE INFO

Article history:
Received 12 April 2011
Received in revised form 25 May 2011
Accepted 26 May 2011
Available online 6 June 2011

Keywords:
W–ZrC composites
Displacive compensation of porosity (DCP)
Microstructure
Mechanical property
Ablation resistance

ABSTRACT

Tungsten–zirconium carbide composites were fabricated at different temperatures by the displacive compensation of porosity (DCP) method, the microstructure, mechanical properties, and ablation resistance were investigated. It was found that no WC phase was left in the composites prepared at 1400 °C, and a few residual W_2C particles were surrounded in W product. Microstructure analyses revealed that zirconium atoms diffused into tungsten carbide to form ZrC and W_2Zr besides carbon diffused into the Zr_2Cu melt. Composites fabricated at 1400 °C had a flexural strength of 356.7 ± 15.2 MPa, an elastic modulus of 193.7 ± 9.8 GPa, a fracture toughness of 7.0 ± 0.7 MPa $m^{1/2}$, and a hardness of 13.6 ± 0.7 GPa. After ablated by an oxyacetylene flame for 30 s, the higher temperature prepared composites had a better ablation resistance, the linear ablation rate was 0.0033 ± 0.0004 mm/s, and the mass ablation rate was 0.0012 ± 0.0001 g/s.

1. Introduction

Tungsten, due to its high melting point, high strength, high thermal conductivity, and low thermal expansion coefficient, is attractive for aerospace applications, such as rocket nozzles and re-entry components [1–4]. Zirconium carbide, for its extremely high melting temperature (3540 °C), relatively low density (ρ[ZrC] = 6.63 g/cm^3, one third of ρ[W]), good ablation resistance [4–6], and being consistent with tungsten [7,8], has been introduced into the refractory metal [4,6,7]. Furthermore, composites of these two materials can improve the flexural strength of tungsten and the fracture toughness of zirconium carbide at elevated temperature [9,10].

The tungsten–zirconium carbide composites have been produced with tungsten and ZrC powders by hot pressing [4,6,9–12], the composites had superior elevated temperature strength, higher elastic modulus, lower density, and lower conductivity compared with the monolithic tungsten, the interdiffusion of Zr and W to form (Zr,W)C solid solution was beneficial to achieving good bond strength of the W/ZrC interface [9]. W–ZrC composites were also produced via in situ reaction sintering by Zhang et al. [13]. In this process, a solid-state reaction between ZrO_2 and WC was used, and ZrC powder was added to adjust the microstructure. Recently, a novel method for preparation the composites, known as the displacive compensation of porosity (DCP) method, was developed by Dickerson and Sandhage et al. [7,14–16]. The DCP method, in which a molten Zr_2Cu alloy infiltrated into and then reacted with a porous WC perform at modest temperatures, was effective and promising for fabricating ZrC/W composites. Zhao studied the wetting of WC by molten Zr_2Cu [17], Amadeh investigated the infiltration parameters on composition of the composites [18], and Lipke fabricated W–ZrC composites with complex geometries using this method [19].

However, there is little information available on the properties of the W–ZrC composites prepared by the DCP method, making such an investigation is necessary and valuable. In this work, we focus on the microstructure, mechanical properties, and ablation resistance of the W–ZrC composites.

2. Experimental procedure

2.1. Raw materials

The porous rigid preforms were prepared with the following commercial materials: WC powder (D50 = 0.45 μm, purity: 99.9%, Xiamen Golden Egret Special Alloy Co., Ltd., China), polycarbosilane (PCS, average molecular weight: 1300, soften point: 210 °C, National University of Defence Technology, China). The WC powder, together with 3 wt.% PCS were mixed in a polypropylene bottle using WC balls and xylene as the grinding media for 2 h. The mixed materials were dried in a plate (400 mm × 300 mm) at room temperature and then granulated using a 100 mesh sieve. The granules were die-pressed at a peak stress of 20 MPa for 5 min to form bars (40 mm × 35 mm × 3.5 mm). The green bars were heated to 1200 °C for 0.5 h in flowing Ar (purity: 99.999%) and then cooled spontaneously to room temperature, the heating rate was 20 °C/min.

The commercial Zr_2Cu ingots (purity: 99.6%, Hunan Rare Earth Metal & Material Institute, Hunan, China), were used as the reactive infiltrant. Zr_2Cu ingots were prepared with spongy Zr pieces (purity: 99.6%) and copper cylinders (purity: 99.99%)

* Corresponding author. Tel.: +86 731 84576441; fax: +86731 84573165.
E-mail address: shoumzh@163.com (S. Zhang).

0925-8388/$ – see front matter © 2011 Elsevier B.V. All rights reserved.
doi:10.1016/j.jallcom.2011.05.105

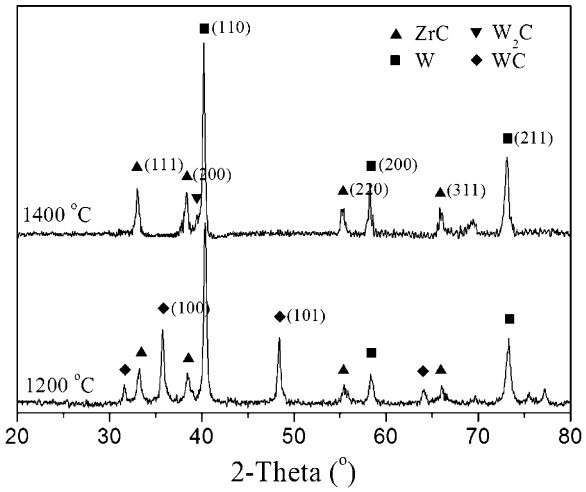

Fig. 1. XRD patterns of the resulting composites prepared at different temperatures.

by arc melting. To allow for homogenization, each ingot was flipped and remelted three times.

2.2. Preparation of W–ZrC composites

Before reactive melt infiltration, pieces of the solid Zr_2Cu ingot were placed on top of the WC preforms within a flat-bottomed graphite crucible (purity: 99.995%, Ø70 mm × 40 mm). The molar ratio of Zr_2Cu:WC used in each experiment was 2–3:1. The furnace atmosphere was a mild vacuum about 20 Pa for all temperatures. The Zr_2Cu-covered preforms were heated to high temperatures for 2 h at 10 °C/min and then cooled spontaneously to room temperature.

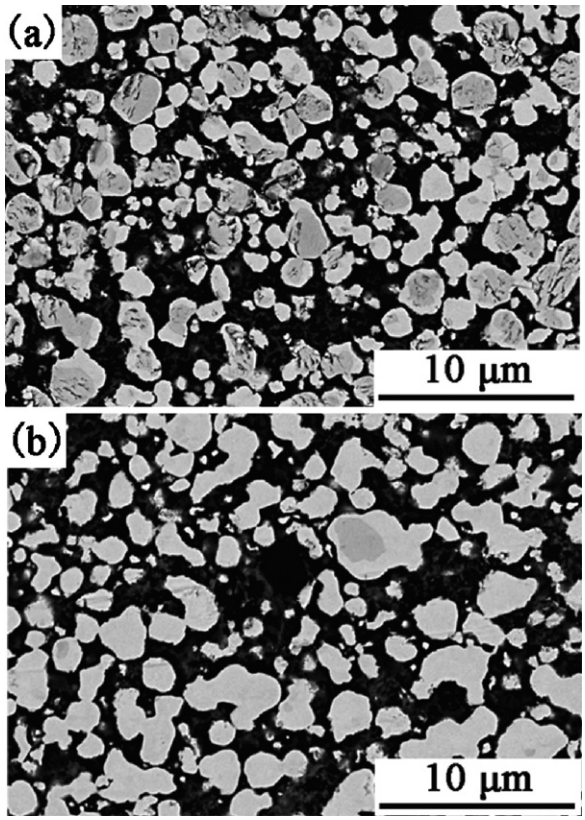

Fig. 3. The BSE images of composites prepared at different temperatures: (a) 1200 °C and (b) 1400 °C.

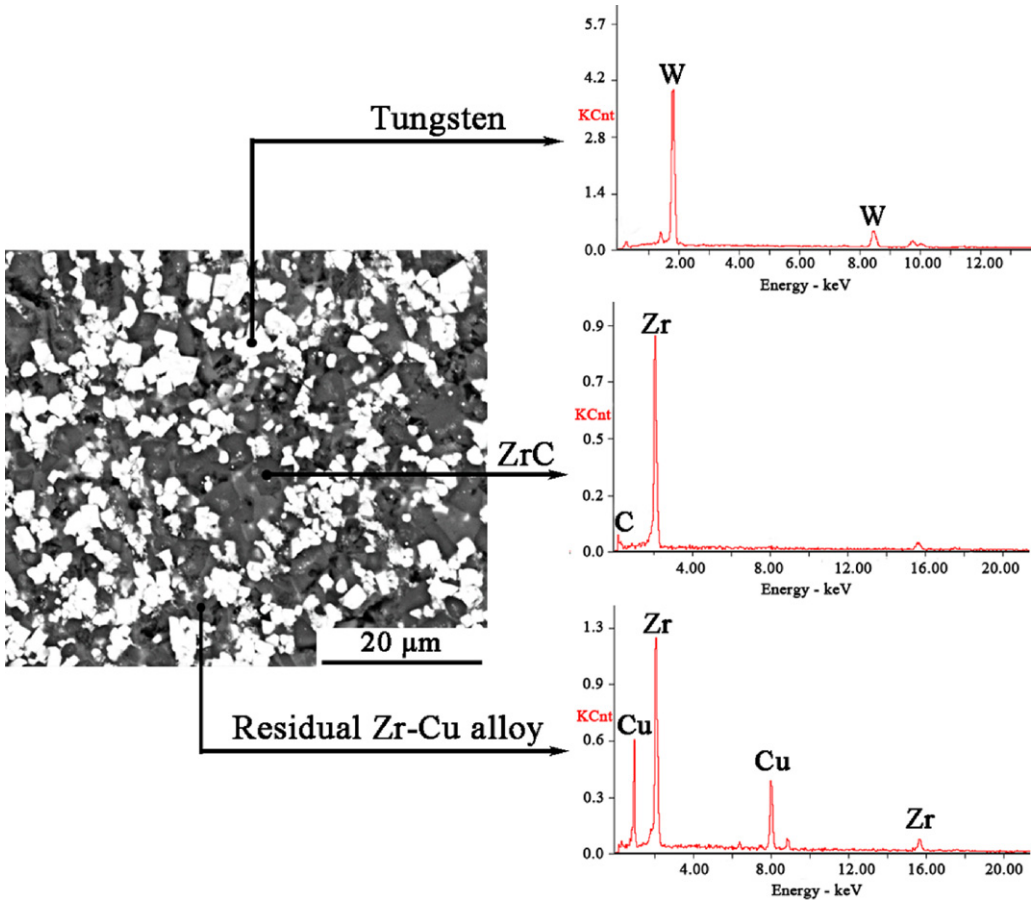

Fig. 2. The backscattered electron image with corresponding EDS analyses on different phases in the composites prepared at 1400 °C.

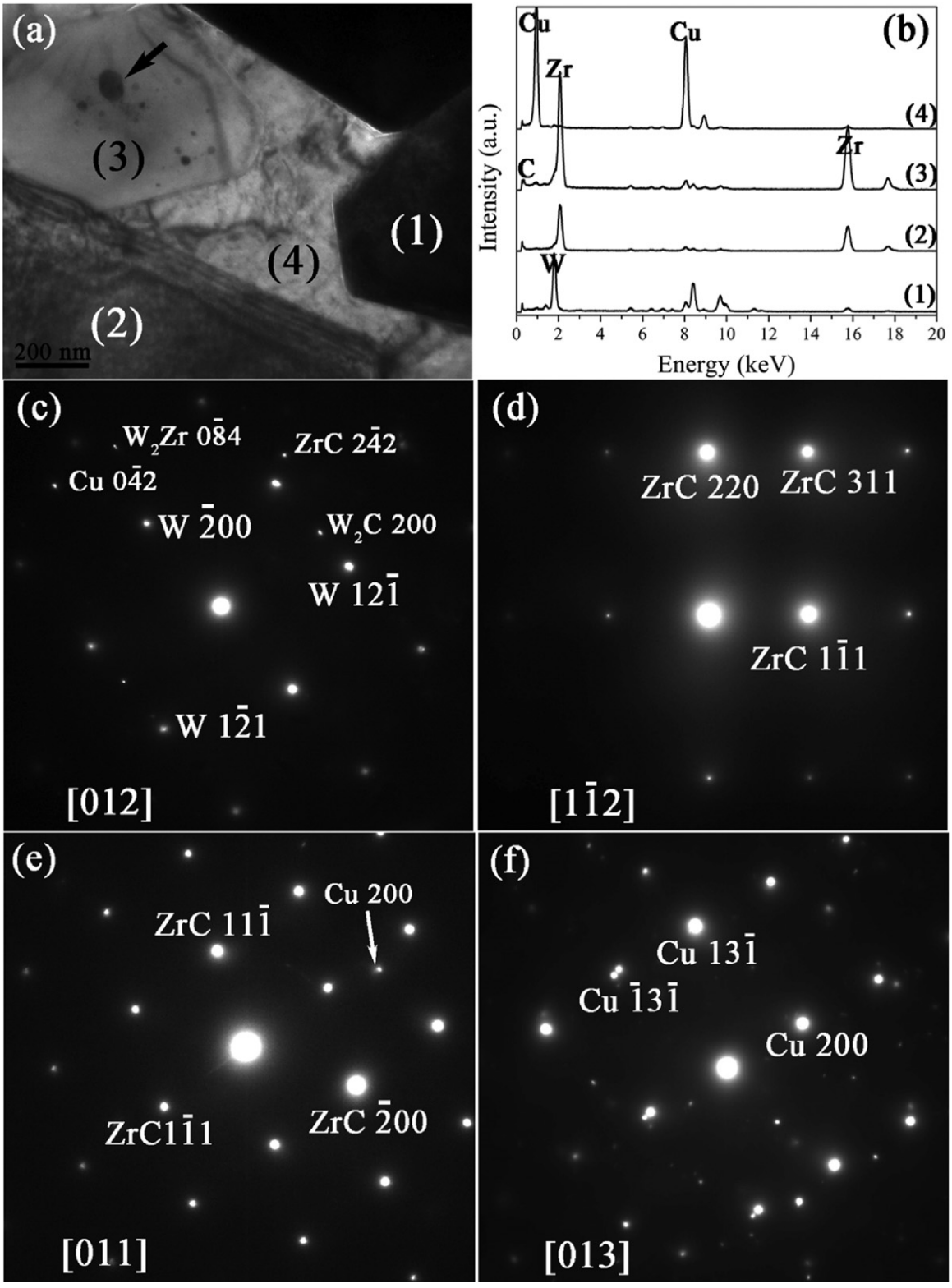

Fig. 4. (a) TEM micrograph of the composite prepared at 1400 °C. (b) EDS analyses of the four parts in the TEM graph. (c)–(f) Selected diffraction patterns relative to part (1)–(4) in (a), respectively.

2.3. Evaluation of the microstructure and properties of the composites

A Rigaku X-Ray Diffractometer was used to carry out X-ray diffraction analysis of the polished cross sections perpendicular to the growth direction. The scanning rate was chosen as 4 °/min. Backscattered electron images of polished cross sections were obtained with Quanta-200, and secondary electron images were obtained with a S4800 FE-SEM. EDAX was performed to determine chemical composition. The TEM sample was prepared by grinding a bulk sample to about 80 μm in thickness and then a 3 mm diameter disc was cut out. The disc was subsequently dimpled and ion milled. Images and selected area electron diffraction (SAED) patterns were obtained with a transmission electron microscope (TEM; JEOL, Tokyo, Japan; JEM-2010F). Image analysis was conducted to determine the composite phase content (ImageJ 1.42q, National Institutes of Health, Bethesda, MD).

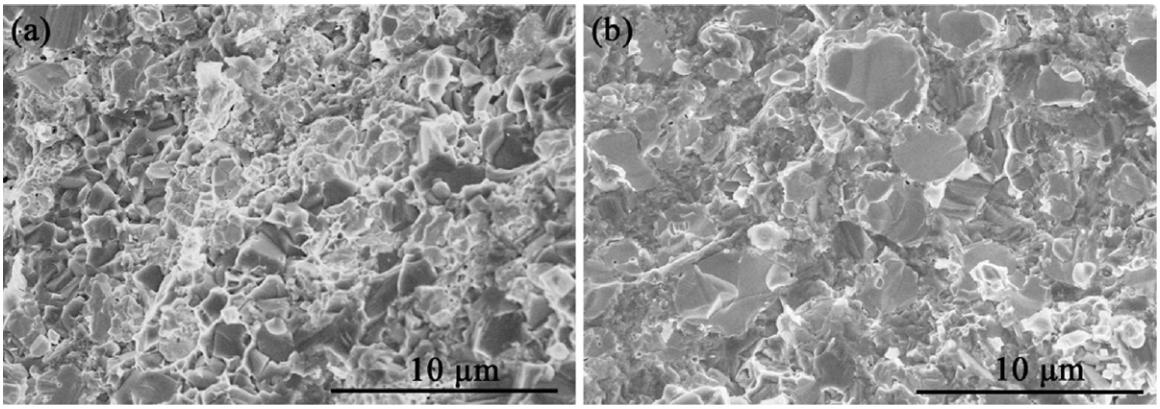

Fig. 5. Fracture surface of W–ZrC composites prepared at different temperatures: (a) 1200 °C and (b) 1400 °C.

Flexural strength was measured using a three-point-bending test on five specimens of 3.0 mm × 4.0 mm × 40 mm with 30 mm span and a crosshead speed of 0.5 mm/min. Elastic modulus was calculated by the bending method based on the Chinese Standard GB/T 10700-2006. Fracture toughness was evaluated by a single-edge notched-beam test with a 24 mm span and a crosshead speed of 0.05 mm/min, three samples were tested. The test bars, 3.0 mm × 6.0 mm × 40 mm, were notched by electromachining with a 0.2-mm-diameter Mo line. The notches were about 0.2 mm in width and 3.0 mm in depth. All samples were gotten by the electric discharge machining, ground, polished with a series of diamond pastes to a surface finish of 0.5 μm, and bevelled the edges. Microhardness was determined on smoothly polished surfaces using Vickers indentation at a load of 1 kg and a dwell time of 15 s, the reported hardness values were the average of five indentation measurements.

The ablation properties were tested using an oxyacetylene flame in a self-made facility according to GJB323A-96 Ablation Standard. The pressures of oxygen and acetylene were 0.4 MPa and 0.095 MPa, respectively. The ablation gun with a gun-point diameter of 2 mm was ignited firstly, the flux of acetylene and oxygen were turned to 1.116 m^3/h and 1.512 m^3/h, respectively. The ablation gun was then moved perpendicular to the sample surface. The distance between the tip of the gun and the top of the sample was 10 mm. The exposure time under the torch flame was 30 s. The heat flux was calculated from the heat absorbed by water flowing through a calorimeter and the value was 4152.9 kW/m^2. At least three samples with a dimension of 30 mm × 30 mm × 4 mm were examined in each test. The linear ablation rate and the mass ablation rate were calculated by the thickness change and the weight change before and after the test for each sample [6].

3. Results and discussion

3.1. Microstructure

Two composites have been prepared at different temperatures, XRD patterns are shown in Fig. 1. Peaks of tungsten and zirconium carbide were observed in both the two diffractions. There was WC left in composites prepared at 1200 °C, while the process temperature increased to 1400 °C, the residual WC grains reacted to form W_2C [20]. The comparison of peak intensity has been used to determine the crystalline texture [21,22]. Compared with the two XRD patterns, the peak intensities of the ZrC products had no obvious difference, the intensities of W(1 1 0) were about the same, but the gap of peak intensity of W(2 0 0) was bigger than that of W(2 1 1). The differences indicated that the degrees of crystallization of the three crystal faces might be differently sensitive to the temperature. The preferred crystallization face was W(1 1 0) in which there were the densest atoms, the W(2 0 0) crystal face grew better at last with the process temperature increased. The different sensitivity might be ascribed to the different density of atoms in each crystal face. Diffraction angles of all crystal faces were shifted to lower angle positions when the temperature increased, which means the lattice parameters of W and ZrC increased, and there were some other atoms solved in W and ZrC grains.

The backscattered electron image and EDS analysis of polished cross-sections of the composites prepared at 1400 °C are shown in Fig. 2. Combined with the EDS analysis and the XRD patterns, the brightest parts were ascribed as the tungsten phase, the dark parts were ZrC phase, and the gaps between W grains and ZrC grains were filled with the residual Zr–Cu alloy (grey parts). The W phase was discontinuous, which came from the raw WC powder and was different from the continuous W matrix in the hot-pressed W–ZrC composites reported by Roosta and Zhang [8,10]. The size of the W particles was about 1–4 μm, and there should be about 19% volume decrease theoretically when 1 mol WC reacted to form 1 mol W. Because carbon atoms in the ZrC product also came from the raw WC material, the ZrC grains surrounded the W phase. The carbide appeared in regular polygons, which means that each ZrC particle was a single crystal, and it can play an important role in strengthening. The W particles and ZrC particles were found distributing asymmetrically, the reason was that small particles got together and grew up for long time heating.

The composites prepared at different temperatures were compared in Fig. 3. The contrast in the micrographs was intentionally changed to better show the residual tungsten carbide. It was found that the residual reactant was a grey core surrounded by a relatively bright coating. After the interface reaction, the unreacted WC particle was surrounded by the W layer, subsequently carbon atoms in the core diffused out in the further reaction [16,19]. When the temperature increased, the diffusion became easier, and there should be fewer remnants. Image analysis revealed that there was about 18.1 vol.% residual reactant in the composites prepared at 1200 °C, and the value was much smaller (about 6.9 vol.%) in the composites prepared at 1400 °C.

Composites fabricated at 1400 °C were examined with TEM. The EDS analysis revealed that there were W, Zr, Cu, C elements in part (1), the diffraction pattern indicated tungsten was the main phase, and W_2C, W_2Zr, and ZrC were present in the W grain. The composition indicated that there might be another reaction mechanism that zirconium atoms had diffused into the WC particle besides carbon atoms diffused out. The diffraction pattern in Fig. 4(e) showed that there were some Cu atoms dissolved in the ZrC grain, and nano scale inclusions were also found in the grain, which has been found by Zou et al. [23]. Meanwhile, Fig. 4(d) revealed that part (2) was a pure ZrC grain. The C/Zr ratio in part (3) was much lower than that in part (2) from the EDS analyses, and the size was smaller, so the ZrC in part (3) was carbon-deficient and newly formed [24], its growth could be understood from the comparison of the two parts. When carbon atoms diffused into the Zr–Cu melt, they bonded with Zr atoms to form ZrC_x, and copper atoms took up the lacunas in the unsaturated ZrC_x grains. Carbon atoms in ZrC_x became saturated with the reaction time prolonged, and copper was extruded out at the same time. After the reaction finished, most copper was expelled out of the body

Table 1
The mechanical properties of W–ZrC composites prepared by the DCP method.

Infiltration temperature (°C)	Flexural strength (MPa)	Elastic modulus (GPa)	Fracture toughness (MPa $m^{1/2}$)	Vickers hardness (GPa)
1200	288.4 ± 12.3	179.9 ± 15.9	5.3 ± 1.1	8.6 ± 0.4
1400	356.7 ± 15.2	193.7 ± 9.8	7.0 ± 0.7	13.6 ± 0.7

[15,19], a litter alloy (part (4)) was left because it was surrounded by W and ZrC.

3.2. Mechanical properties and fracture characteristics

Mechanical properties of the W–ZrC composites prepared by the DCP method were listed in Table 1. Compared with the composites prepared by hot pressing and reactive sintering [9,13], the properties were not very good. One reason was that the content of tungsten was much smaller, the maximum content was 38 vol.% theoretically when all WC powder reacted to form W and ZrC, while the content was at least 60 vol.% in the composites prepared by hot pressing or reactive sintering. The other reason was that the tungsten phase distributed in isolated particles, while the tungsten powder was sintered together in the composites prepared by hot pressing and reactive sintering. Composites fabricated at 1400 °C had better properties than the ones prepared at 1200 °C, this could be explained by the differences in the microstructure between the two composites. The composites prepared at 1200 °C had more WC particles left, the particles were stuck together by the pyrolysates

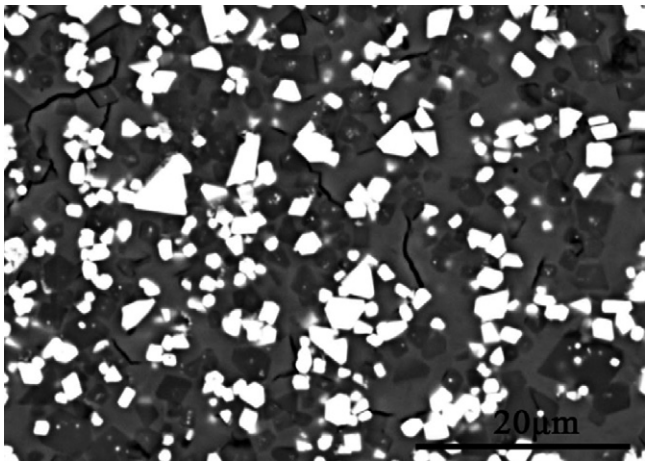

Fig. 6. Crack paths during the fracture toughness measurement of W–ZrC composites prepared at 1400 °C.

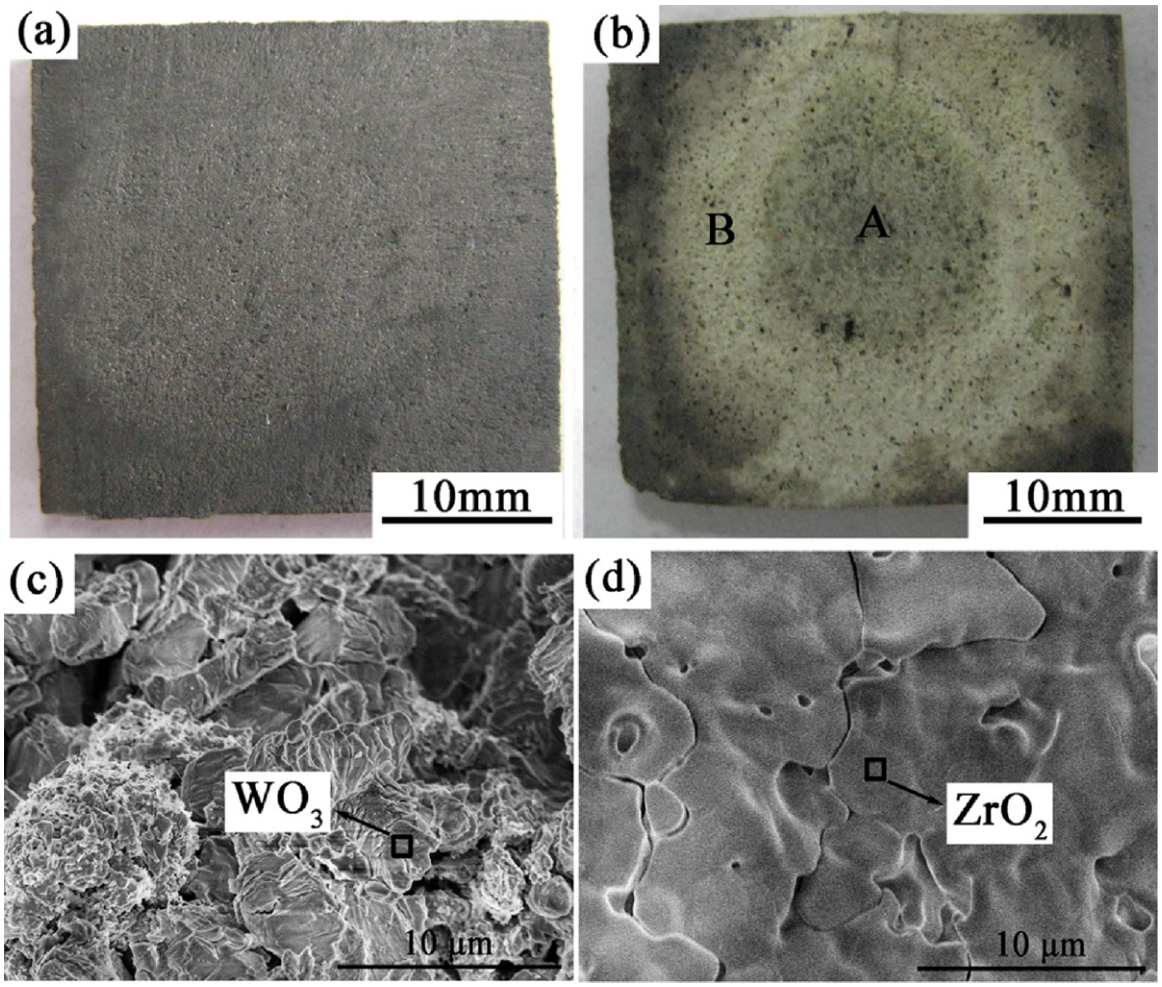

Fig. 7. Morphologies of the ablated W–ZrC composites prepared at 1400 °C: optical images of the sample before (a) and after (b) ablation; SEM micrographs relative to A (c) and B (d) in (b).

Table 2
The ablation properties of W–ZrC composites prepared at different temperatures by the DCP method.

Infiltration temperature (°C)	Linear ablation rates (mm/s)	Mass ablation rates (g/s)
1200	0.0087 ± 0.0006	0.0013 ± 0.0002
1400	0.0033 ± 0.0004	0.0012 ± 0.0001

of PCS (Fig. 3(a)), so there were more bugs in the composites. Another reason was that there were more tungsten particles sintered together in the higher temperature prepared composites (Fig. 3(b)), this may be beneficial to improve the mechanical properties.

The fracture surface of composites fabricated at 1200 °C was coarser than that of the composites prepared at 1400 °C (Fig. 5). The fracture mode was different in the two composites, it was intergranular in the low temperature fabricated composites, while the processing temperature increased, the interface binding strength increased, the fracture mode translated to be transgranular. The crack path is shown in Fig. 6. All were short cracks, and distributed in the residual alloy. The extending of the cracks was stuck by the W grains and was deflected by the ZrC grains, the zigzag feature of the cracks was beneficial to the improvement of the toughness [10].

3.3. Ablation resistance

Since the composites are used to produce high temperature components, in which ablation is the main cause of material failure, the oxyacetylene flame ablation test was done to estimate the resistance. The ablation properties are listed in Table 2. The linear and mass ablation rates were obtained by the dimension and weight change per second of the samples before and after ablation test. As can be seen, composites prepared at 1400 °C had a better ablation resistance.

The macrographic pictures of the composite prepared at 1400 °C before and after ablation are shown in Fig. 7. The ablated surface with a light green layer showed two different parts (A and B) which were magnified in Fig. 7(c) and (d). During the ablation process, ZrC would react with oxygen in the flowing gas to form ZrO_2 [25,26], dense ZrO_2 layer were found at the brim region which could enhance the ablation resistance. When it cooled down, ZrO_2 transformed from tetragonal phase to monoclinic phase, which leaded to a large volume change. At the center of the ablated sample, ZrO_2 spalled off the surface for this reason.

4. Conclusions

W–ZrC composites were fabricated at 1200 °C and 1400 °C by the displacive compensation of porosity (DCP) method. Composites prepared at 1400 °C had no WC left, only a few W_2C was found to be surrounded by the tungsten. Besides carbon atoms diffused out, zirconium atoms in the melt have diffused into the WC grains to form ZrC and W_2Zr. Composites prepared at 1400 °C had better mechanical properties and ablation resistance. They had a flexural strength of 356.7 ± 15.2 MPa, an elastic modulus of 193.7 ± 9.8 GPa, a fracture toughness of 7.0 ± 0.7 MPa $m^{1/2}$, and a Vickers hardness of 13.6 ± 0.7 GPa. After the composites were ablated by an oxyacetylene flame for 30 s, the higher temperature prepared composites had a better linear ablation rate of 0.0033 ± 0.0004 mm/s and a better mass ablation rate of 0.0012 ± 0.0001 g/s.

Acknowledgements

The authors sincerely thank the support from the National Natural Science Foundation of China (Nos. 90916002 and 51002186).

References

[1] S.W. Yih, C.T. Wang, Tungsten-sources, Metallurgy Properties and Application, Plenum Press, New York, 1979.
[2] A. Mondal, A. Upadhyaya, D. Agrawal, J. Alloys Compd. 509 (2011) 301–310.
[3] A. Genc, S. Coskun, M.L. Ovecoglu, J. Alloys Compd. 497 (2010) 80–89.
[4] G.M. Song, Y.J. Wang, Y. Zhou, J. Mater. Sci. 36 (2001) 4625–4631.
[5] W. Sun, X. Xiong, B.Y. Huang, G.D. Li, H.B. Zhang, Z.K. Chen, X.L. Zheng, Carbon 47 (2009) 3365–3380.
[6] G.M. Song, Y.J. Wang, Y. Zhou, Mater. Character. 50 (2003) 293–303.
[7] M.B. Dickerson, P.J. Wurm, J.R. Schorr, W.P. Hoffman, P.G. Wapner, K.H. Sandhage, J. Mater. Sci. 39 (2004) 6005–6015.
[8] M. Roosta, H. Baharvandi, Int. J. Refract. Met. Hard Mater. 28 (2010) 587–592.
[9] G.M. Song, Y.J. Wang, Y. Zhou, Mater. Sci. Eng. A 334 (2002) 223–232.
[10] T.Q. Zhang, Y.J. Wang, Y. Zhou, G.M. Song, Mater. Sci. Eng. A 527 (2010) 4021–4027.
[11] T.Q. Zhang, Y.J. Wang, Y. Zhou, G.M. Song, Int. J. Refract. Met. Hard Mater. 28 (2010) 498–502.
[12] Y.J. Wang, H.X. Peng, Y. Zhou, G.M. Song, Mater. Sci. Eng. A 528 (2011) 1805–1811.
[13] S.C. Zhang, G.E. Hilmas, W.G. Fahrenholtz, J. Am. Ceram. Soc. 90 (2007) 1930–1933.
[14] P. Kumar, K.H. Sandhage, J. Mater. Sci. 34 (1999) 5757–5769.
[15] M.B. Dickerson, R. Snyder, K.H. Sandhage, J. Am. Ceram. Soc. 85 (2002) 730–732.
[16] Z. Grzesik, M.B. Dickerson, K.H. Sandhage, J. Mater. Res. 18 (2003) 2135–2340.
[17] Y.W. Zhao, Y.J. Wang, Y. Zhou, P. Shen, Scripta Mater. 64 (2011) 229–232.
[18] M. Adabi, A. Amadeh, Int. J. Refract. Met. Hard Mater. 29 (2011) 31–37.
[19] D.W. Lipke, Y.S. Zhang, Y.J. Liu, B.C. Church, K.H. Sandhage, J. Eur. Ceram. Soc. 30 (2010) 2265–2278.
[20] C.M. Fernandes, A.M.R. Senos, Int. J. Refract. Met. Hard Mater. 29 (2011) 405–418.
[21] Y. Yang, S. Jayaramana, D.Y. Kim, G.S. Girolami, J.R. Abelsona, J. Cryst. Growth 294 (2006) 389–395.
[22] D.W. Ni, G.J. Zhang, Y.M. Kan, Y. Sakka, Scripta Mater. 60 (2009) 615–618.
[23] L.H. Zou, N. Wali, J.M. Yang, N.P. Bansal, D. Yan, Int. J. Appl. Ceram. Technol. 8 (2011) 329–341.
[24] A.F. Guillermet, J. Alloys Compd. 217 (1995) 69–89.
[25] Y.G. Wang, X.J. Zhu, L.T. Zhang, L.F. Cheng, Ceram. Int. 37 (2011) 1277–1283.
[26] X.M. Hou, K.C. Chou, J. Alloys Compd. 509 (2011) 2395–2400.